March, 1982

GROUP VELOCITY AND REFLECTION PHENOMENA IN NUMERICAL APPROXIMATIONS OF HYPERBOLIC EQUATIONS: A SURVEY

R. Vichnevetsky

DCS-TR-116

Department of Computer Science
Rutgers University
New Brunswick, New Jersey 08903

(To appear in the Journal of the Franklin Institute)

ABSTRACT

Recent analyses of spurious phenomena near interfaces and boundaries of numerical approximations of hyperbolic equations have produced a host of interesting, concrete results which are reviewed in this paper.

What characterizes these analyses is that they rely on tools of mathematical physics, in particular in the systematic use of Fourier transforms and the concept of sinusoidal wave propagation this leads to a description of numerical inaccuracy in terms of dispersion, and a description of spurious numerical solutions in terms of wave packets and group velocities.

It is in providing the mathematics needed to describe spurious reflection at numerical boundaries and at interfaces in mesh refinement that the most applied results of this theory are obtained.

1. INTRODUCTION

Recent analyses of spurious phenomena near interfaces and boundaries of numerical approximations of hyperbolic equations have produced a host of interesting, concrete results which are reviewed in this paper.

What characterizes these analyses is that they rely on tools of mathematical physics, in particular in the systematic use of Fourier transforms and the concept of sinusoidal wave propagation. This leads to a description of numerical inaccuracy in terms of dispersion, and a description of spurious numerical solutions in terms of wave packets and group velocities.

It is in providing the mathematics needed to describe spurious reflection at numerical boundaries and at interfaces in mesh refinement that the most applied results of this theory are obtained. This is illustrated in the last four sections of the paper.

Since hyperbolic equations describe propagation in continuous media, it is the case that their numerical discretizations describe propagation in the periodic structure obtained when a continuum is discretized and modeled by what is called a lumped parameters system. One finds in the development of applied mathematics and physics a large and interesting succession of uses of such semi-discrete models. One of the first is possibly that of Newton [Principia, Book II, (1686)], in his attempts to find a physical model for the propagation of sound.

In the first half of the eighteenth century, Johann and Daniel Bernouilli used similar discrete models to describe vibrating strings, and d'Alembert used this approach, passing to the limit, to "invent" (in his own words) partial differential equations.

The relation of trigonometric series with propagation in continua and in their discrete models was well known in the eighteenth century. This was used, among others, by Euler and Lagrange. The name of Fourier, which was later to be attached to those series, came when he proved that their applicability was less restricted than was believed, while he was applying them, also using discrete models at first, to solve the diffusion equation which he had just discovered.

Crystal lattices offer a physical example of discrete conducting media. Sinusoidal wave propagation through such structures and many of the attending developments in Fourier analysis had been well established by the end of the nineteenth century.

Many of these developments are reported in Brillouin (1946). Numerical discretizations of partial differential equations have created new families of similar periodic structures. It thus comes as no surprise that applying Fourier analysis to study their properties proves to be a very fruitful endeavor.

An important property of discrete media is that they are dispersive; that is, the phase velocity of sinusoidal waves depends on frequency. The concept of group velocity, which plays a primordial role in signal and energy propagation through dispersive media emerged in the nineteenth century. It had been used conceptually by Hamilton (1839), was known to Rayleigh (Theory of Sound - 1877) and was fully investigated in the early part of this century with publications of Sommerfeld (1912, 1914) in prominent place. Here also, this classical result from mathematical physics has provided the starting point for the investigation of a host of interesting aspects of propagation properties of numerical discretizations of hyperbolic equations.

2. SEMI-DISCRETIZATIONS

Consider as a model of hyperbolic equations the simple advection equation:

$$\frac{\partial U}{\partial t} + c \frac{\partial U}{\partial x} = 0 \qquad (1)$$

and a regular division of the x axis:

$$x_n = n.h \; ; \quad n = 0, \pm 1, \pm 2, \cdots \qquad (2)$$

The set notation:

$$\{ U_n(t) \}$$

is used to describe semi-discrete functions which are meant to approximate U :

$$U_n(t) \simeq U(x_n, t) \quad \text{for each n} \qquad (3)$$

We shall examine two basic methods of approximation, namely

a) that obtained with classical finite differences:

$$\frac{dU_n}{dt} = -c \left(\frac{U_{n+1} - U_{n-1}}{2h} \right) \qquad (4\text{-a})$$

b) that obtained with the linear finite-element Galerkin method:

$$\frac{1}{6} \left(\frac{dU_{n-1}}{dt} + 4 \frac{dU_n}{dt} + \frac{dU_{n+1}}{dt} \right) = -c \left(\frac{U_{n+1} - U_{n-1}}{2h} \right) \qquad (4\text{-b})$$

and analyze propagation properties of the corresponding solutions. A remark about (4) is in order: these are semi-discrete approximations (or semi-discretizations) of equation (1). Since numerical calculations are fully discrete, (time is discretized as well), the question of the validity of (4) as models arises. But it is the case that when fully discrete calculations are carried out with a courant number $(c\cdot\Delta t/h)$ which is reasonably small (say $\leq .1$) then the error introduced by time discretization becomes negligible, and (4) are indeed legitimate models of the computational process.

We note in passing that those models are sometimes called "method of lines" approximations. The term was first coined by Russian mathematicians in the 1940's. See e.g. Faddeyeva (1949).

While the analysis in this paper is restricted to semi-discrete models of computational processes, most results extend easily to full discretizations (See [32]).

3. ENERGY

An important property of solutions of hyperbolic equations is that they obey an energy conservation principle. E.g., if $U(x,t)$ is a solution of the advection equation (1), then

$$\frac{d}{dt}\|U\|_2^2 \equiv \frac{d}{dt}\int |U(x,t)|^2 dx$$
$$= \left[-c\,U^2\right]_{-\infty}^{\infty} \qquad (5)$$

Mathematical tractability is simplified when $\|U\|_2^2$ is finite, i.e., when U is in $\mathcal{L}_2$. This implies that $U(\pm\infty,t)=0$ thus that (5) vanishes and conservation of energy

$$\|U\|_2^2 = \text{constant} \qquad (6)$$

follows. Multiplying each equation of (4) by U_n and summing over all n shows that a discrete form of energy is conserved by numerical solutions that are in ℓ_2, viz.

$$\|U_n\|_2^2 \equiv h\sum_n U_n^2 = \text{constant} \qquad (7a)$$

in the finite difference approximation (4-a), and

$$\|U_n^*\|_2^2 \equiv \frac{h}{3}\sum_n \left(2U_n^2 + U_n U_{n+1}\right) = \text{constant} \qquad (7b)$$

with the linear finite element Galerkin approximation (4-b).

Distribution of energy on the x axis is described by the local energy density functions

$$|U(x,t)|^2 \tag{8}$$

in the exact case, by

$$U_n^2 \tag{9-a}$$

and

$$\frac{1}{3}(2U_n^2 + U_n \cdot U_{n+1}) \tag{9-b}$$

in the discrete cases. Energy propagation for solutions of the exact equation (1) is a simple collective displacement at the uniform velocity C:

$$|U(x,t)|^2 = |U(x-ct,0)|^2 \tag{10}$$

But energy propagation in the discrete equations is not as simple. The discrete approximations introduce spurious dispersion, and energy propagation is no more a uniform displacement.

The mathematics which describe wave propagation in dispersive media are based on Fourier analysis. Some of the basic concepts that are relevant will be described in the following sections.

4. t-FOURIER ANALYSIS

We define the t-Fourier transform of $U_n(t)$ as

$$\hat{U}_n(\Omega) = \int_{-\infty}^{\infty} U_n(t)\, e^{-i\Omega t}\, dt \tag{11}$$

and that of $U(x,t)$ as

$$\hat{U}(x,\Omega) = \int_{-\infty}^{\infty} U(x,t)\, e^{-i\Omega t}\, dt \tag{12}$$

If U is a solution of (1), then

$$\hat{U}(x,\Omega) = \hat{U}(0,\Omega)\, e^{-i\Omega x/c} \tag{13}$$

For each Ω, this describes harmonic (or sinusoidal) wave propagation at a constant amplitude

$$|\hat{U}(x,\Omega)| = |\hat{U}(0,\Omega)| \tag{14}$$

at a spatial frequency

$$\omega = \Omega/c \tag{15}$$

with a wavelength

$$\lambda = 2\pi/\omega = 2\pi c/\Omega \tag{16}$$

To find the analog of this in the semi-discretizations, we seek fundamental solutions of (4), i.e., solutions for which the ratio

$$\hat{E}(\Omega) \equiv \frac{\hat{U}_{n+1}}{\hat{U}_n} \tag{17}$$

is independent of n

It is found that $\hat{E}$ must satisfy a characteristic equation,

derived from (4), which is in the two cases considered, with $\overline{\Omega} \equiv \Omega h/c$:

a) finite differences:

$$\hat{E}^2 + 2i\overline{\Omega}\,\hat{E} - 1 = 0 \qquad (18\text{-a})$$

b) finite elements:

$$(3 + i\overline{\Omega})\,\hat{E}^2 + 4i\overline{\Omega}\,\hat{E} - (3 - i\overline{\Omega}) = 0 \qquad (18\text{-b})$$

These are algebraic equations of second degree. Both semi-discretizations thus admit two types of fundamental solutions, which we denote as $\{p_n\}$ and $\{q_n\}$ and which satisfy, respectively:

$$\hat{p}_{n+1}(\Omega) / \hat{p}_n(\Omega) = \hat{E}_1(\Omega) \qquad (19)$$

$$\hat{q}_{n+1}(\Omega) / \hat{q}_n(\Omega) = \hat{E}_2(\Omega) \qquad (20)$$

where $\hat{E}_1(\Omega)$ and $\hat{E}_2(\Omega)$ are the two roots of (18) (See Table 1). We may state this as:

Property 1

Solutions of the semi-discretizations (4) may be expressed as the sum:

$$\{u_n\} = \{p_n\} + \{q_n\} \qquad (21)$$

of two fundamental types. Their respective Fourier transforms:

$$\hat{p}_n(\Omega) = \hat{p}_0(\Omega) \cdot [\hat{E}_1]^n \qquad (22)$$

and

$$\hat{q}_n(\Omega) = \hat{q}_0(\Omega) \cdot [\hat{E}_2]^n \qquad (23)$$

describe the different propagation properties that apply to each.

When $|\hat{E}(\Omega)| = 1$, then (17) describes sinusoidal wave propagation at a conserved amplitude, with a phase velocity

$$c^*(\Omega) = -\Omega h / \angle \hat{E}(\Omega) \qquad (24)$$

and a wavelength

$$\lambda(\Omega) = 2\pi c^*(\Omega)/\Omega \qquad (25)$$

This occurs for frequencies $|\Omega|$ which are below a cut-off frequency Ω_c which is equal to c/h with finite differences, and to $\sqrt{3}\,c/h$ with finite elements.

An analytic description of these functions is given in table 1, and they are illustrated in figures 1 and 2.

By contrast with the exact case, numerical phase velocities are found to be frequency dependent. This introduces what is known as dispersion in the numerical approximations. Propagation properties in a dispersive medium can be significantly different from propagation properties in a non-dispersive medium. In particular, energy and signal propagate at what is known as the group velocity (not the phase velocity c): the corresponding mathematics are given in Section 6 and 7 below.

In the particular case of the numerical approximations (4), it shall be found that while phase velocities are always positive, group velocities of solutions corresponding to the second root of the characteristic equation (18) are negative. Thus, numerical solutions exist that carry energy and signal in a direction which is opposite to the flow. Such solutions are clearly spurious.

	FINITE DIFFERENCES	LINEAR FINITE-ELEMENT GALERKIN
CHARACTERISTIC RATIO $\hat{E}(\Omega) = \hat{u}_{n+1} / \hat{u}_n$	$\hat{E}_{1,2} = -i\bar{\Omega} \pm \sqrt{1-\bar{\Omega}^2}$	$\hat{E}_{1,2} = \dfrac{-2i\bar{\Omega} \pm \sqrt{9-3\bar{\Omega}^2}}{3+i\bar{\Omega}}$
CUT-OFF FREQUENCY	$\Omega_c = c/h$ $\omega_c = \pi/2h$ $\lambda_c = 4h$	$\Omega_c = \sqrt{3}c/h$ $\omega_c = 2\pi/3h$ $\lambda_c = 3h$
OLUTIONS OF $\{p_n\}$ TYPE: SPATIAL FREQUENCY	$\lvert\omega_1\rvert < \omega_c = \pi/2h$	$\lvert\omega_1\rvert < \omega_c = 2\pi/3h$
PHASE VELOCITY	$c_1^* = c\bar{\Omega}/\arcsin(\bar{\Omega})$ $= c \cdot \sin(\omega_1 h)/\omega_1 h$	$c_1^* = c\bar{\Omega}/[\arctan(2\bar{\Omega}/\sqrt{9-3\bar{\Omega}^2}) + \arctan(\bar{\Omega}/3)]$ $= c\cdot[\sin(\omega_1 h)/\omega_1 h]\cdot[3./(2+\cos(\omega_1 h))]$
WAVELENGTH	$\lambda_1 = 2\pi h/\arcsin(\bar{\Omega})$	$\lambda_1 = 2\pi h/[\arctan(2\bar{\Omega}/\sqrt{9-3\bar{\Omega}^2} + \arctan(\bar{\Omega}/3)]$
OLUTIONS OF $\{q_n\}$ TYPE: SPATIAL FREQUENCY	$\frac{\pi}{2h} < \lvert\omega_2\rvert \leq \frac{\pi}{h}$	$\frac{2\pi}{3h} < \lvert\omega_2\rvert \leq \frac{\pi}{h}$
PHASE VELOCITY	$c_2^* = c\bar{\Omega}/[\pi - \arcsin(\bar{\Omega})]$ $= c\cdot\sin(\omega_2 h)/\omega_2 h$	$c_2^* = c\bar{\Omega}/[\pi - \arctan(2\bar{\Omega}/\sqrt{9-3\bar{\Omega}^2}) + \arctan(\bar{\Omega}/3)]$ $= c[\sin(\omega_2 h)/\omega_2 h]\cdot[3/(2+\cos(\omega_2 h))]$
WAVELENGTH	$\lambda_2 = 2\pi h/[\pi - \arcsin(\bar{\Omega})]$	$\lambda_2 = 2\pi h/[\pi - \arctan(2\bar{\Omega}/\sqrt{9-3\bar{\Omega}^2}) + \arctan(\bar{\Omega}/3)]$

Table 1. PROPERTIES OF SINUSOIDAL SOLUTIONS

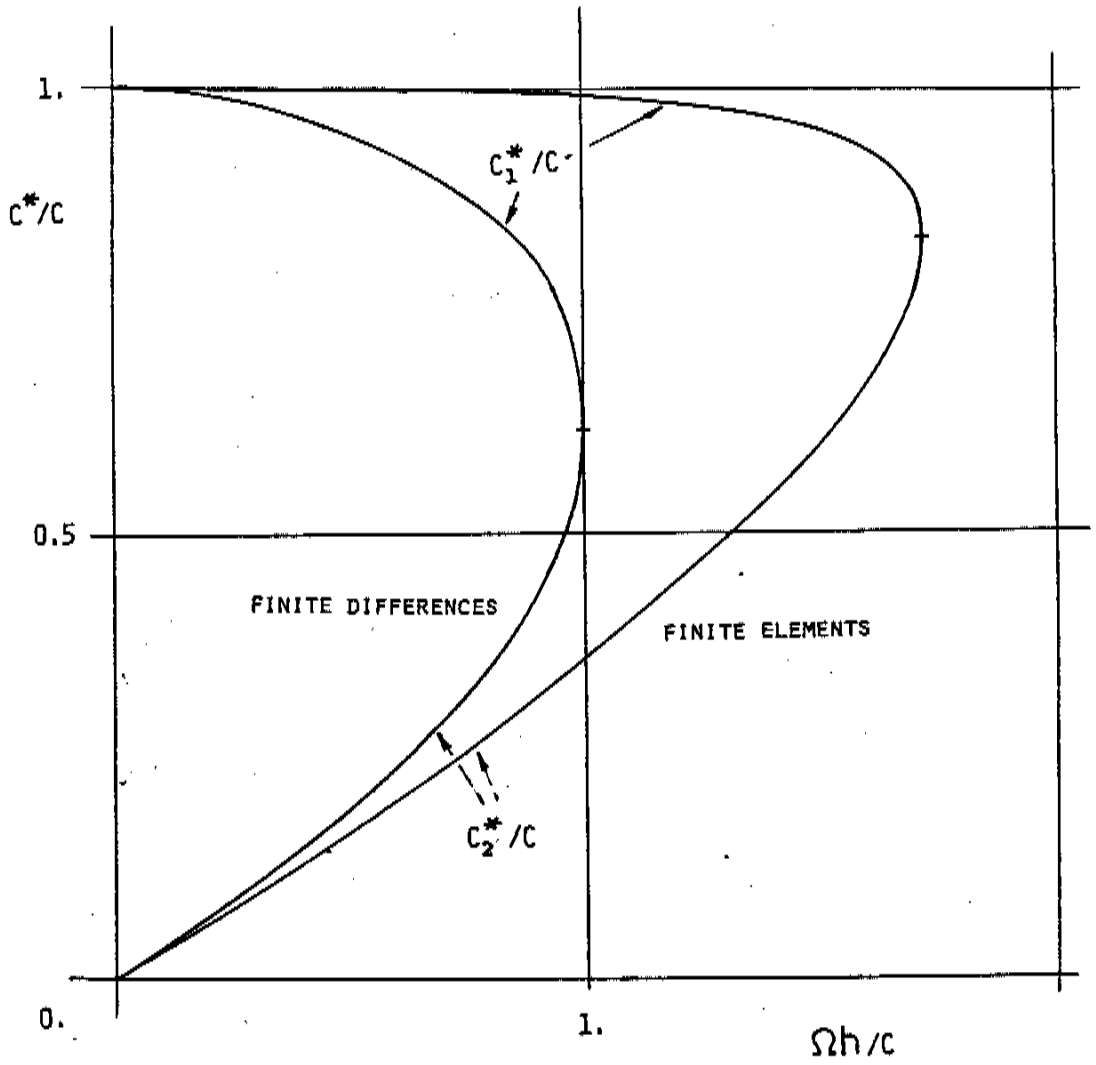

Figure 1: Numerical phase velocity of finite difference and finite element approximations of $u_t + c\, u_x = 0$

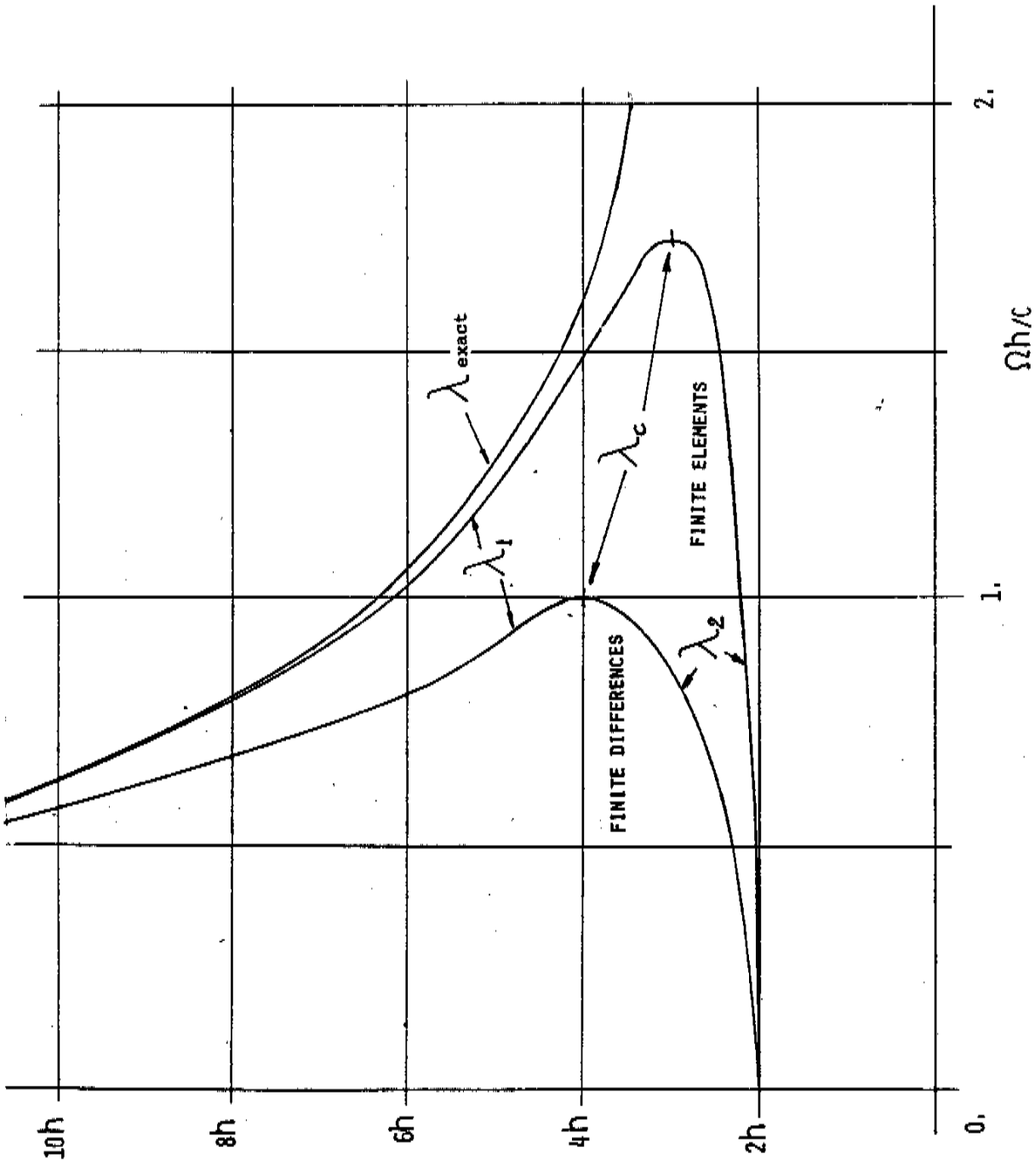

Figure 2: Wavelength of finite difference and finite element approximations of $U_t + cU_x = 0$

5. χ-FOURIER ANALYSIS

Other aspects of propagation are obtained with the use of χ-Fourier Transforms:

The χ-Fourier transform of $U(x,t)$ is defined as

$$\hat{U}(\omega,t) \equiv \int_{-\infty}^{\infty} U(x,t)\, e^{-i\omega x}\, dx \qquad (26)$$

Similarly, the expression

$$\overline{U}(\omega,t) \equiv h \sum_{n} U_n\, e^{-i\omega x_n} \qquad (27)$$

defines the discrete χ- Fourier transform of $\{U_n\}$. Below cut off, harmonic waves are sinusoidal in both x and t. The correspondence between ω and Ω is simply:

$$\omega = \Omega / c^*(\Omega) \qquad (28)$$

Applying this to the analytic results of the previous sections reveals the following properties: (See also figure 3)

Property 2

The χ-Fourier transforms of fundamental solutions of the $\{p_n\}$ and $\{q_n\}$ type have non overlapping support in ω, viz

$$0 \leq \omega_1 < \omega_c < \omega_2 \leq \pi/h \qquad (29)$$

where ω_1 are frequencies corresponding to $\{p_n\}$, ω_2 are frequencies corresponding to $\{q_n\}$, and ω_c is the spatial frequency corresponding to the cut-off temporal frequency Ω_c

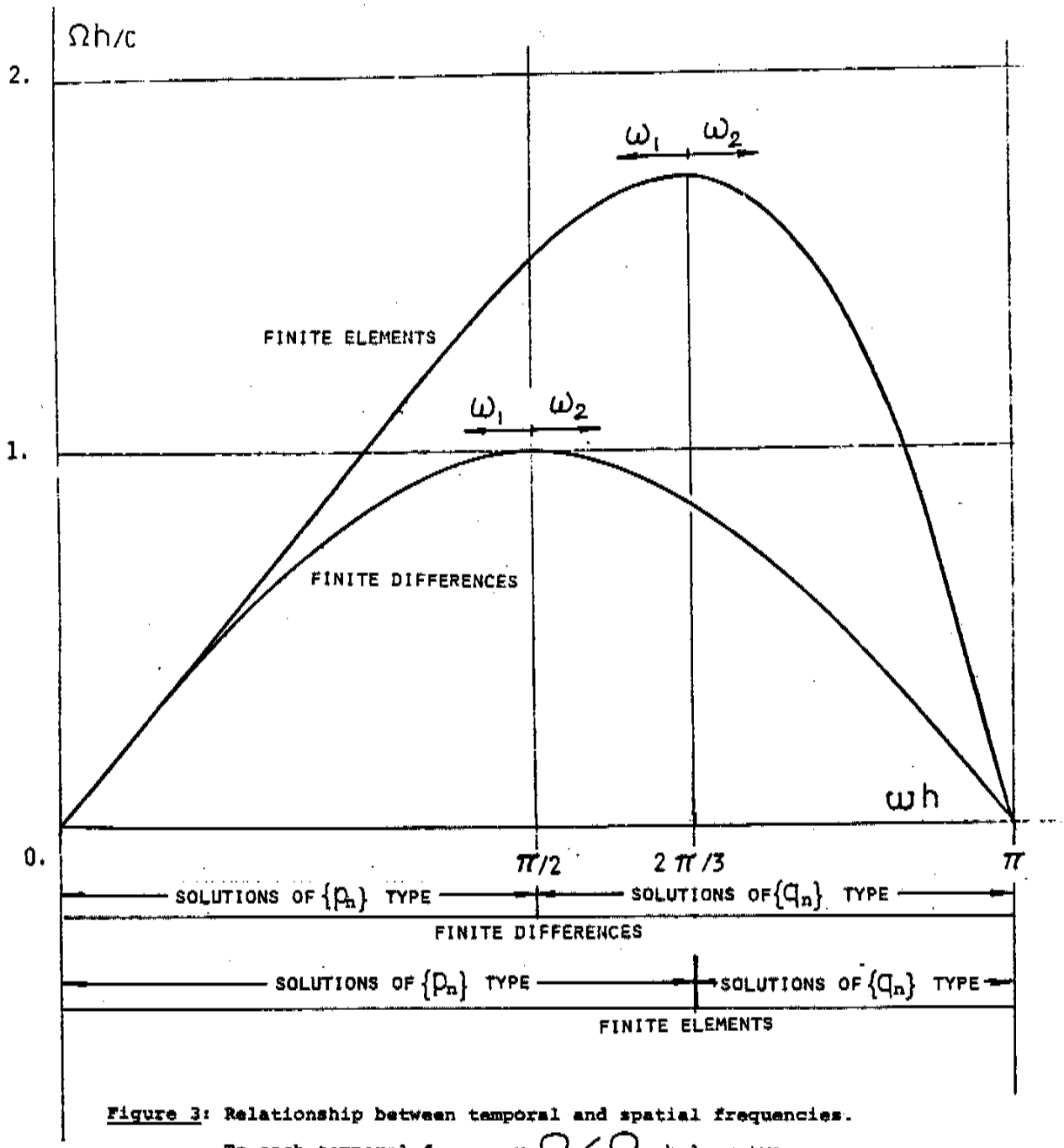

Figure 3: Relationship between temporal and spatial frequencies. To each temporal frequency $\Omega < \Omega_c$ belong two spatial frequencies ω_1 and ω_2, which correspond to one another in reflection phenomena.

Property 3

Numerical solutions of $\{p_n\}$ *and* $\{q_n\}$ *types have wavelength in* (λ_c, ∞) *and* $(2h, \lambda_c)$ *respectively, where* λ_c *is the wavelength of solutions corresponding to* Ω_c

The energy of $U(x,t)$ may be expressed in terms of its Fourier transform $\hat{U}(\omega,t)$ through Parseval's relation as:

$$\|U\|_2^2 = \int |\hat{U}(\omega,t)|^2 \frac{d\omega}{2\pi} \tag{30}$$

Conservation of energy results here from the fact that:

$$\frac{\partial}{\partial t} |\hat{U}(\omega,t)| = 0 \tag{31}$$

for solutions of the advection equation (1).

The energy of the discrete function $\{u_n(t)\}$ is expressed by the appropriate form of Parseval's relation as (see [23] or [32] for details)

$$\|u_n\|_2^2 = \int_{-\pi/h}^{\pi/h} |\overline{u}(\omega,t)|^2 \frac{d\omega}{2\pi} \tag{32}$$

$$= \int_0^{\pi/h} |\overline{u}(\omega,t)|^2 \frac{d\omega}{\pi}$$

The discrete Fourier transform $\overline{u}(\omega,t)$ may be decomposed in its two components

$$\overline{u}(\omega,t) = \overline{p}(\omega,t) + \overline{q}(\omega,t) \tag{33}$$

Then, from (29) results the simple and interesting energy separation property:

$$\|u_n\|_2^2 = \int_0^{\pi/h} |\overline{u}(\omega,t)|^2 \frac{d\omega}{\pi}$$

$$= \int_0^{\omega_c} |\overline{p}(\omega,t)|^2 \frac{d\omega}{\pi} + \int_{\omega_c}^{\pi/h} |\overline{q}(\omega,t)|^2 \frac{d\omega}{\pi} \qquad (34)$$

or,

Property 4

The energy of numerical solutions $\{u_n\}$ *satisfies the separation principle*

$$\|u_n\|_2^2 = \|p_n\|_2^2 + \|q_n\|_2^2 \qquad (35)$$

And it easily shown that each of these two components of the energy remain constant.

6. ENERGY PROPAGATION AND GROUP VELOCITY

To study energy propagation in numerical solutions one must introduce the concept of "wave group" or "wave packet" as it is used in classical physics. It is by analyzing the propagation of wave packets in dispersive media that the concept of group velocity appears.

A (conservative), dispersive medium is one where sinusoidal waves propagate (without amplitude decay) at a phase velocity c^* which is frequency dependent.

That is, propagation is described by:

$$V(x,t) = \int \hat{V}(\omega,0)\, e^{i\omega(x - c^*(\omega)t)}\, \frac{d\omega}{2\pi} \tag{36}$$

A wave packet is a single frequency sinusoidal wave, modulated by a slowly varying envelope as illustrated in figure 4. The mathematical description of a wave packet of frequency β at some initial time $t = 0$ is

$$V(x,0) = A(x,0)\, e^{i\beta x} \tag{37}$$

If the Fourier transform of the envelope $A(x,0)$ is $\hat{A}(\omega,0)$, the assumption that A varies slowly is equivalent to assuming that $\hat{A}$ is band limited:

$$|\hat{A}(\omega,0)| = 0 \quad \text{when} \quad |\omega| > \gamma; \quad \gamma \ll \beta \tag{38}$$

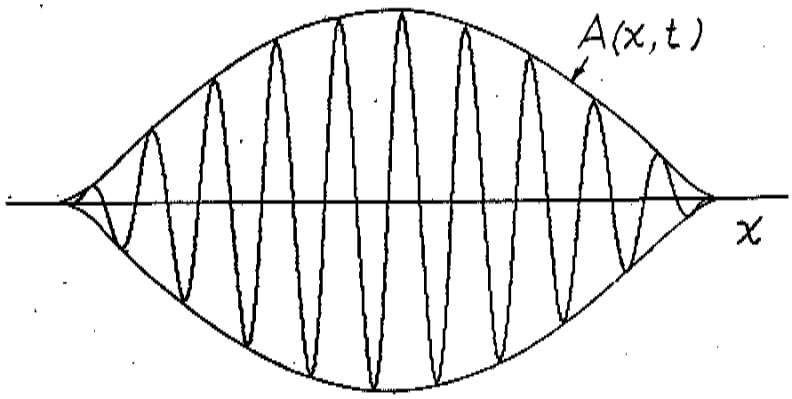

Figure 4 Typical wave packet, consisting of short wavelengths oscillations modulated by a slowly varying envelope.

The Fourier transform of (37) is obtained by application of the convolution rule:

$$\hat{V}(\omega,0) = \hat{A}(\omega,0) \otimes 2\pi\delta(\omega-\beta) = \hat{A}(\omega-\beta) \tag{39}$$

Applying then (36) to find the time-history of $V(x,t)$ we obtain:

$$V(x,t) = \int \hat{A}(\omega-\beta)\, e^{i\omega(x - c^*(\omega)\cdot t)}\, \frac{d\omega}{2\pi} \tag{40}$$

Since, from (38), the intergrand is non zero only in the narrow band $\omega \in (\beta-\gamma, \beta+\gamma)$, we may use Taylor's theorem to rewrite the above as

$$V(x,t) = \tag{41}$$

$$\int \hat{A}(\omega-\beta)\, e^{i\omega x}\, e^{-i[\beta c^*(\beta) + (\omega-\beta)\mathcal{V}(\beta)]t}\, \frac{d\omega}{2\pi}$$

where

$$\mathcal{V}(\omega) = \frac{d}{d\omega}\left(\omega\, c^*(\omega)\right) \tag{42}$$

This expression for $V(x,t)$ may now be rewritten as:

$$V(x,t) =$$

$$= \int \hat{A}(\omega-\beta)\, e^{i(\omega-\beta)(x-\mathcal{V}(\beta)t)}\, e^{i\beta(x-c^*(\beta)t)}\, \frac{d\omega}{2\pi}$$

$$= A(x-\mathcal{V}(\beta)t, 0)\; e^{i\beta(x-c^*(\beta)t)} \qquad (43)$$

which expresses that the wave packet propagates as:

- a sinusoidal function of frequency β, moving without distortion at the phase velocity $c^*(\beta)$
- modulated by an envelope $A(x-\mathcal{V}(\beta).t)$ moving without distortion at the velocity $\mathcal{V}(\beta)$ called group velocity.

The energy of the wave packet

$$\int |A(x-\mathcal{V}t,0).\, e^{i\omega(x-c^*t)}|^2\, dx = \int |A(x,t)|^2\, dx \qquad (44)$$

is constant. This energy, which is concentrated in the wave packet, thus travels with the packet at the group velocity $\mathcal{V}(\beta)$. I.e., the group velocity is also the velocity at which energy is propagated in the dispersive medium.

The group velocity may also be derived from $c^*(\Omega)$. Since

$$\mathcal{V} = \frac{d}{d\omega}(\omega\, c^*(\omega)) = \frac{d\Omega}{d(\Omega/c^*(\Omega))} \qquad (45)$$

we find

$$\frac{1}{\mathcal{V}(\Omega)} = \frac{d}{d\Omega}\left(\frac{\Omega}{c^*(\Omega)}\right) \qquad (46)$$

7. GROUP VELOCITY OF NUMERICAL SOLUTIONS

Applying these results to numerical solutions of the advection equation, i.e.:

$$\frac{1}{\gamma_1} = \frac{d}{d\Omega}\left(\frac{\Omega}{C_1^*(\Omega)}\right) \tag{47}$$

and

$$\frac{1}{\gamma_2} = \frac{d}{d\Omega}\left(\frac{\Omega}{C_2^*(\Omega)}\right) \tag{48}$$

produces the functions given in Table 2, and illustrated in Figure 5.

Important to note is that to fundamental solutions of $\{p_n\}$ type correspond positive group velocities, while to solutions of $\{q_n\}$ type correspond negative group velocities.

We may state:

Property 5

Numerical wave packets of $\{p_n\}$ *type have a positive group velocity. For smooth numerical solutions,* $(\omega h \to 0 \text{ or } \lambda \to \infty)$ *this group velocity approaches* $+C$

Smooth numerical solutions converge to the exact solution of (1), with both group and phase velocity approaching the exact value C.

Property 6

Numerical wave packets of $\{q_n\}$ *type have a negative group velocity - For the highest frequency* $\left(\omega = \frac{\pi}{h} \text{ or } \lambda = 2h\right)$ *this group velocity equals* $-C$ *in the finite difference case, and* $-3C$ *in the finite element case ,*

These are important results: while phase velocity analyses would suggest that solutions of $\{p_n\}$ and $\{q_n\}$ type both propagate in the direction of flow (since both phase velocities are positive) the group velocity analysis reveals that solutions of $\{q_n\}$ type carry information upstream. In reflection phenomena, solutions of $\{p_n\}$ type, arriving at a discontinuity will be partially reflected, obviously in the opposite direction, as solutions of $\{q_n\}$ type:

It is thus sometimes useful to refer to $\{p_n\}$ as "forward" or "downstream" solutions and to $\{q_n\}$ as "backward" or "upstream" solutions. (See also Figure 3.)

	FINITE DIFFERENCES	LINEAR FINITE-ELEMENT GALERKIN
DISCRETE ENERGY	$\|U_n\|_2^2 = h\sum_n U_n^2$	$\|U_n^*\|_2^2 = \frac{h}{3}\sum_n (2U_n^2 + U_n U_{n+1})$
DISCRETE ENERGY: FOURIER INTEGRAL FORM	$\|U_n\|_2^2 = \int_{-\frac{\pi}{h}}^{\frac{\pi}{h}} \|\bar{U}(\omega,t)\|^2 \frac{d\omega}{2\pi}$	$\|U_n^*\|_2^2 = \int_{-\frac{\pi}{h}}^{\frac{\pi}{h}} \|\bar{U}(\omega,t)\|^2 \left(\frac{2+\cos(\omega h)}{3}\right) \frac{d\omega}{2\pi}$
GROUP VELOCITY - IN TERMS OF SPATIAL FREQUENCY	$\mathcal{V} = c\cdot\cos(\omega h)$	$\mathcal{V} = 3c\,\frac{1+2\cos(\omega h)}{(2+\cos(\omega h))^2}$
- IN TERMS OF TEMPORAL FREQUENCY	$\mathcal{V}_1 = c\sqrt{1-\bar{\Omega}^2}$	$\mathcal{V}_1 = 3c\left(\frac{1+\frac{1}{9}\bar{\Omega}^2}{2+\sqrt{1-\frac{1}{3}\bar{\Omega}^2}}\right)\sqrt{1-\frac{1}{3}\bar{\Omega}^2}$
	$\mathcal{V}_2 = -c\sqrt{1-\bar{\Omega}^2}$	$\mathcal{V}_2 = 3c\left(\frac{1+\frac{1}{9}\bar{\Omega}^2}{-2+\sqrt{1-\frac{1}{3}\bar{\Omega}^2}}\right)\sqrt{1-\frac{1}{3}\bar{\Omega}^2}$

Table 2. ENERGY AND ENERGY PROPAGATION

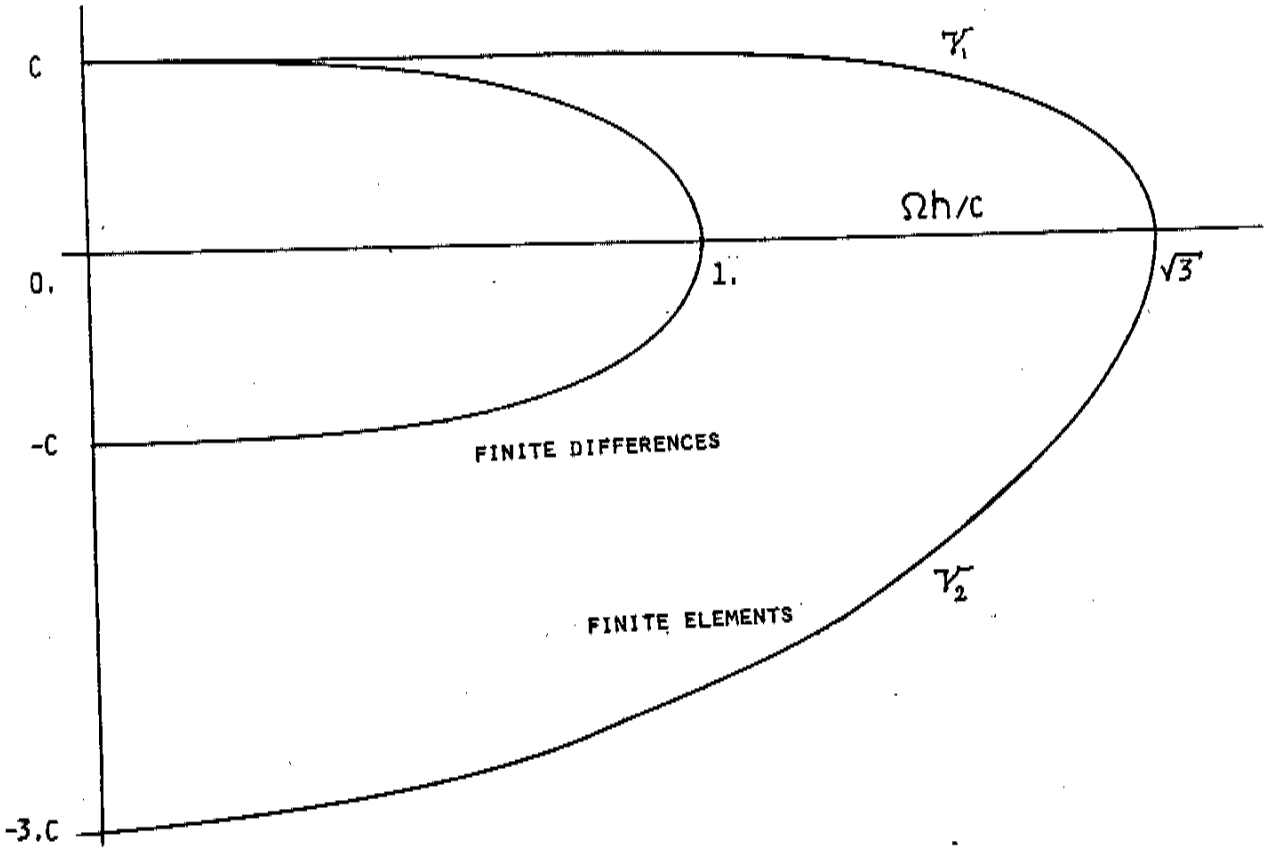

Figure 5: Group velocity of finite difference and finite element approximations of $U_t + cU_x = 0$
Positive group velocities correspond to solutions of $\{p_n\}$ type while negative group velocities correspond to solutions of $\{q_n\}$ type.

8. CUT OF FREQUENCY

When $|\Omega| > \Omega_c$, then $|\hat{E}_1(\Omega)| < 1.$ and $|\hat{E}_2(\Omega)| > 1.$ Solutions which are sinusoidal in time at those frequencies are no more constant - amplitude sinusoidal in space (as they were when $|\Omega| \leqslant \Omega_c$). They have an envelope which decays exponentially with $\varkappa$ for solutions of $\{p_n\}$ type, and with $(-\varkappa)$ for solutions of $\{q_n\}$ type. Such solutions cannot be generated by initial conditions on an infinite domain. They may, however, occur near boundaries and mesh discontinuities as shall be illustrated in examples below.

We also see (from Table 2 and Figure 5) that to the cut off frequency Ω_c correspond numerical solutions with a vanishing group velocity. It is thus the case that solutions with $|\Omega| \geqslant \Omega_c$ cannot transport energy. Reference to and/or analysis of such solutions may be found in Roache (1972), Browning, Kreiss and Oliger (1973), Vichnevetsky (1980), Vichnevetsky and Bowles (1982).

Similar results to those obtained with the group velocity theory may be derived from a completely different approach:

Let u_n be relabelled as v_n for energy odd numbered point. Then (4-a) - (4-b) may be rewritten as

a) finite differences:

$$\frac{du_n}{dt} = -c\left(\frac{v_{n+1} - v_{n-1}}{2h}\right)$$

(n even)

$$\frac{dv_n}{dt} = -c\left(\frac{u_{n+1} - u_{n-1}}{2h}\right) \qquad (50a)$$

(n odd)

b) finite elements;

$$\frac{1}{6}\left(\frac{dv_{n-1}}{dt} + 4\frac{du_n}{dt} + \frac{dv_{n+1}}{dt}\right) = -c\left(\frac{v_{n+1} - v_{n-1}}{2h}\right)$$

(n even)

$$\frac{1}{6}\left(\frac{du_{n-1}}{dt} + 4\frac{dv_n}{dt} + \frac{du_{n+1}}{dt}\right) = -c\left(\frac{u_{n+1} - u_{n-1}}{2h}\right) \qquad (50b)$$

(n odd)

These are found to be consistent approximations, when $h \to 0$, of systems of first order equations which become, after transformation to their characteristic form:

$$\left.\begin{aligned} \frac{\partial w_1}{\partial t} + c\frac{\partial w_1}{\partial x} &= 0 \\ \frac{\partial w_2}{\partial t} - c\frac{\partial w_2}{\partial x} &= 0 \end{aligned}\right\} \qquad (51a)$$

and

$$\left.\begin{aligned} \frac{\partial w_1}{\partial t} + c\frac{\partial w_1}{\partial x} &= 0 \\ \frac{\partial w}{\partial t} - 3c\frac{\partial w_2}{\partial x} &= 0 \end{aligned}\right\} \qquad (51b)$$

respectively, where w_1 and w_2 are the new dependent variables:

$$w_1(x,t) = (u+v)/2$$
$$w_2(x,t) = (u-v)/2 \qquad (52)$$

and

$$u(x,t) = w_1 + w_2$$

The characteristic velocity of $w_2(x,t)$ in (51) is observed to be $(-c)$ and $(-3c)$ in the 2 cases considered. The fact that this characteristic velocity is precisely equal to the group velocity $v\left(\frac{\pi}{h}\right)$ in the x-Fourier analysis is no coincidence, but a reflection of the fact that both express an identical result. Indeed, $w_1(x,t)$ and $w_2(x,t)$ represent the smooth and oscillatory part (of period $\lambda = 2h$) of $u(x,t)$, as illustrated in figure 6. The smooth part is analogous to a wave packet with β near 0, and the oscillatory part to wave packets with β near π/h

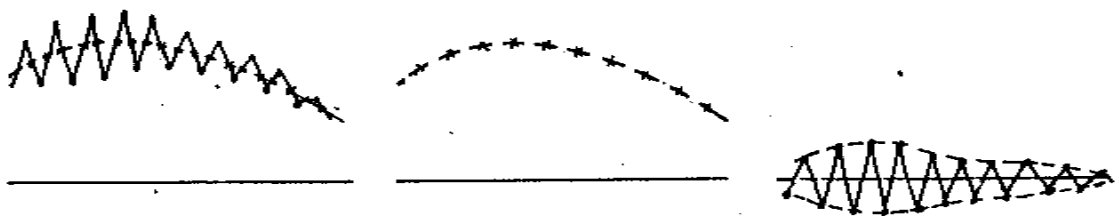

NUMERICAL SOLUTION WITH OSCILLATIONS = SMOOTH PART OBTAINED BY JOINING MID-POINTS + OSCILLATORY PART = COMPLETE SOLUTION MINUS SMOOTH PART

$$u = \frac{u+v}{2} + \frac{u-v}{2}$$

Figure 6

10. PROPAGATION IN TWO DIMENSIONS

The analysis is easily extended to two dimensions. A simple model equation is then

$$\frac{\partial U}{\partial t} + c_x \frac{\partial U}{\partial x} + c_y \frac{\partial U}{\partial y} = 0$$

describing advection by the vector flow velocity

$$\mathbf{c} = \begin{bmatrix} c_x \\ c_y \end{bmatrix}$$

Numerical discretization on a square or rectangular grid then results in numerical phase velocities for sinusoidal solutions which depend on direction as well as frequency. I.e., the approximation introduces a spurious dispersion which is anisotropic (*cf.* Birkhoff and Dougalis (1975), and Vichnevetsky and Bowles (1982) in which numerical phase velocities are given for a variety of discretizations).

Group velocities and illustrations of propagation of two-dimensional wave packets may be found in Trefethen (1982).

11. REFLECTION AT A DOWNSTREAM BOUNDARY

We are now equipped to solve a number of problems having to do with the behavior of numerical solutions near discontinuities of the computational domain

(a) finite differences.

As a first example, consider the non-trivial problem of describing the spurious reflection that occurs near downstream computational boundaries with finite differences. We examine a finite domain $x \in [0, \ell]$ on which the model hyperbolic equation (1) is approximated with (4-a).

At the inlet boundary $x = 0$ we let simply:

$$U_0(t) = U(0,t) \text{ imposed} \tag{53}$$

At the exit boundary $x = \ell$, the equation is replaced by the two-point, upwind approximation:

$$\frac{dU_N}{dt} = -c\left(\frac{U_N - U_{N-1}}{h}\right) \; ; \; U_N \simeq U(\ell, t) \tag{54}$$

Consider now a numerical solution of $\{p_n\}$ type that has been generated by a (band limited in $|\Omega| \leq c/h$) boundary condition and the subsequent reflected solution (of $\{q_n\}$ type) which is generated when $\{p_n\}$ crosses the exit boundary $x_N = \ell$. We have near $x = \ell$:

$$\left.\begin{aligned} \hat{p}_{N-1} &= \hat{p}_N \hat{E}_1^{-1} \\ \hat{q}_{N-1} &= \hat{q}_N \hat{E}_2^{-1} \\ \hat{U}_N &= \hat{p}_N + \hat{q}_N \\ \hat{U}_{N-1} &= \hat{p}_{N-1} + \hat{q}_{N-1} \end{aligned}\right\} \tag{55}$$

Using these expressions in taking the Fourier transform of equation (54), we obtain:

$$i\Omega\left(\hat{p}_N + \hat{q}_N\right) = -\frac{c}{h}\left[\hat{p}_N\left(1-\hat{E}_1^{-1}\right) + \hat{q}_N\left(1-\hat{E}_2^{-1}\right)\right] \tag{56}$$

whence, solving for $\hat{q}_N/\hat{p}_N \equiv \rho(\Omega)$ (called the reflection ratio) results in (figure 7):

$$\rho(\Omega) = -\frac{1-\sqrt{1-(\Omega h/c)^2}}{1+\sqrt{1-(\Omega h/c)^2}} = -\frac{1-\sqrt{1-(\Omega/\Omega_c)^2}}{1+\sqrt{1+(\Omega/\Omega_c)^2}} \tag{57}$$

Ideally, $\rho(\Omega)$ should be equal to zero, since it expresses the amount of spurious reflection occuring at the boundary.

The incident and reflected solutions in $\mathcal{H}_N$ are expressed analytically, exactly, by the Fourier transforms:

$$p_N(t) = \int \hat{p}_N(\Omega)\, e^{i\Omega t}\, d\Omega/2\pi \tag{58}$$

$$= \int_{-c/h}^{c/h} \hat{U}(0,\Omega)\left[\hat{E}_1(\Omega)\right]^N d\Omega/2\pi$$

and

$$q_N(t) = \int \hat{p}_N(\Omega)\,\rho(\Omega)\, e^{i\Omega t}\, d\Omega/2\pi \tag{59}$$

$$= \int_{-c/h}^{c/h} \hat{U}(0,\Omega)\,\rho(\Omega)\left[\hat{E}_1(\Omega)\right]^N e^{i\Omega t}\, d\Omega/2\pi$$

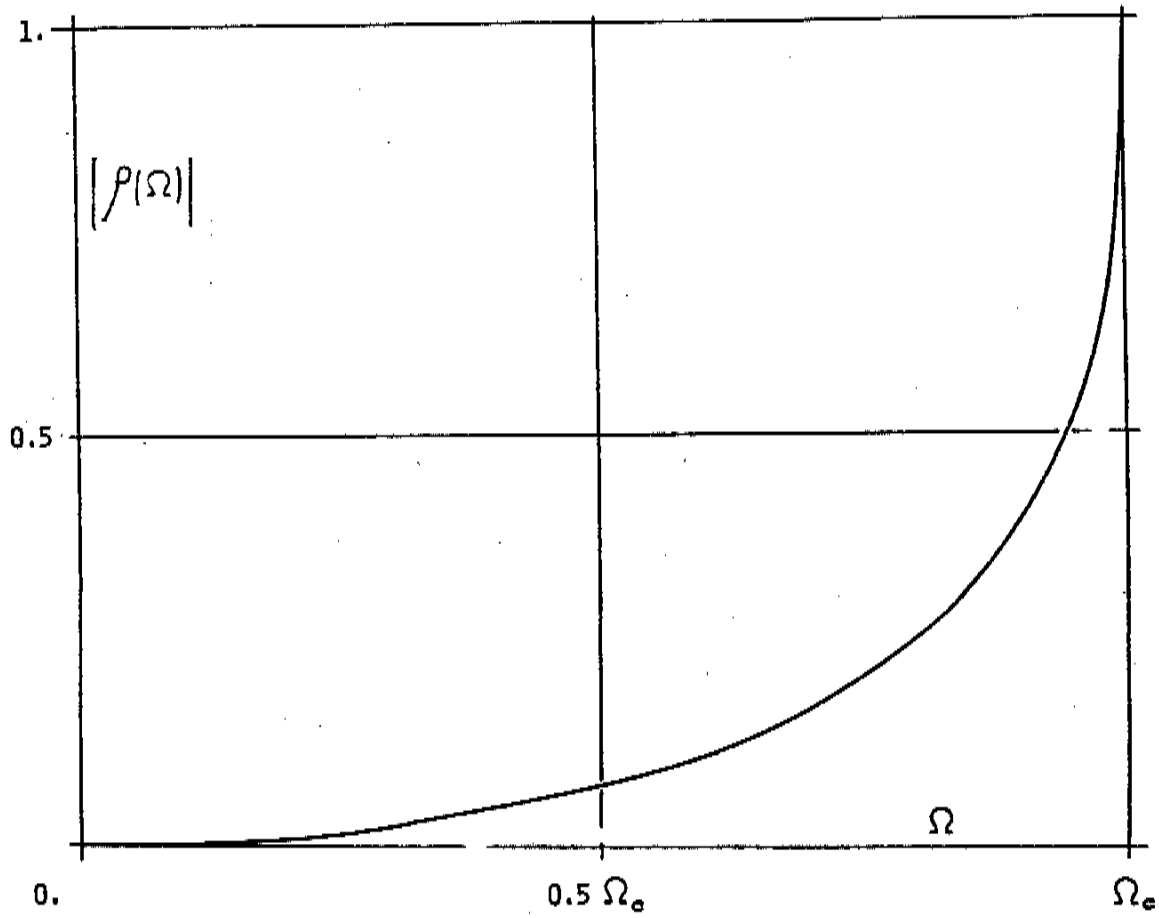

Figure 7: Reflection ratio at a downstream boundary
(finite difference and finite element cases)

Convergence may be analyzed by expanding (58)-(59) in Taylor series, while letting $h \to 0$ with $Nh = \ell$ and $N \to \infty$ (See [32] for details). It is found that $\{p_n\}$ approximates $\{U(x_n, t)\}$ with an error that converges to zero as $O(h^2)$ and that the amplitude of the reflected solution is also $O(h^2)$.

(b) finite elements

The linear finite element Galerkin treatment of an exit or downstream boundary leads to the equation:

$$\frac{1}{3}\left(\frac{dU_{N-1}}{dt}+2\frac{dU_N}{dt}\right)=-c\left(\frac{U_N-U_{N-1}}{h}\right) \tag{60}$$

In a manner similar to that leading to (57), the reflection ratio at the boundary is found:

$$\rho(\Omega)\equiv\frac{\hat{q}_N(\Omega)}{\hat{p}_N(\Omega)}=\frac{1-\sqrt{1-\frac{1}{3}\left(\frac{\Omega h}{c}\right)^2}}{1+\sqrt{1-\frac{1}{3}\left(\frac{\Omega h}{c}\right)^2}} \tag{61}$$

which may be rewritten in a form analogous to (57) as:

$$\rho(\Omega)=\frac{1-\sqrt{1-(\Omega/\Omega_c)^2}}{1+\sqrt{1-(\Omega/\Omega_c)^2}} \tag{62}$$

where Ω_c is here the finite element cut-off frequency $\Omega_c=\sqrt{3}c/h$

Convergence rate analysis shows in this case that $\{p_n\}$ approximates $\{U(x_n,t)\}$ with an error which goes to zero as $O(h^4)$ (which is Thomée's superconvergence result). But the reflection ratio $\rho(\Omega)$ and therefore the amplitude of the reflected solution $\{q_n\}$ are only $O(h^2)$ as in the finite difference case (see [28]).

12. REFLECTION AT AN UPSTREAM BOUNDARY

It is commonly, but as we shall see erroneously, assumed that the best way to treat an upstream or inlet boundary is to let the numerical value equal the imposed value, as in (53). What is wrong in this assumption is that it ignores the presence of spurious solutions (of $\{q_n\}$ or $w_2(x,t)$ type) that may have originated inside of the computational domain or at a downstream boundary and that have a negative group velocity. Such spurious solutions are reflected at the boundary by the common treatment, while a better treatment should attempt to absorb them.

To describe the reflection occuring in $x = 0$ with the standard treatment, we simply note (with $U(0,t) = 0$) that when a solution of $\{q_n\}$ type reaches the boundary, we have:

$$\hat{u}_0 = \hat{p}_0 + \hat{q}_0 = 0 \tag{62}$$

and the reflection ratio is thus

$$\rho \equiv \frac{\hat{p}_0}{\hat{q}_0} = -1 \tag{63}$$

I.e., total reflection.

An improved treatment starts from the observation that $U(0,t)$ is meant to affect solutions of $\{p_n\}$ or $w_1(x,t)$ type only.

Thus, what we want is:

$$w_1(0,t) = U(0,t) \tag{64}$$

We may then use the simple approximation (from (52)):

$$w_2(0,t) = \frac{u_0 - u_1}{2} \tag{65}$$

which , in combination with

$$u_0 = w_1(0,t) + w_2(0,t)$$
$$= U(0,t) + \frac{u_0 - u_1}{2}$$

results in

$$u_0(t) = 2U(0,t) - u_1(t) \tag{66}$$

instead of (53). To find the reflection ratio for spurious solutions with this improved treatment of the boundary, we express the Fourier transforms

$$\hat{u}_0 = \hat{p}_0 + \hat{q}_0 \tag{67}$$

$$\hat{u}_1 = \hat{E}_1 \hat{p}_0 + \hat{E}_2 \hat{q}_0 \tag{68}$$

Inserting these in the Fourier transform of (66), with $U(0,t) = 0$ results in:

$$\rho \equiv \frac{\hat{p}_0}{\hat{q}_0} = \frac{1 + \hat{E}_2}{1 + \hat{E}_1} \tag{69}$$

This applies to both the finite difference and the finite element cases. In both, it is found that

$$\rho(\Omega) = O(\Omega h) \tag{70}$$

More on this, and numerical experiments which illustrate the effect of the improvement may be found in [33]

13- MESH REFINEMENT

Mesh refinement is commonly used when a greater accuracy is seeked in some subdomain of the equation. A simple model of mesh refinement is illustrated in figure 8.

The equations that apply at the interface point $x = 0$ are,

a) finite differences:

$$\frac{du_0}{dt} = -c\left(\frac{u_1 - u_{-1}}{h+k}\right) \tag{71a}$$

b) finite elements:

$$\frac{1}{3}\left(\frac{h}{h+k}\right)\left(\frac{du_{-1}}{dt} + 2\,\frac{du_0}{dt}\right) + \frac{1}{3}\left(\frac{k}{h+k}\right)\left(2\,\frac{du_0}{dt} + \frac{du_1}{dt}\right) = -c\left(\frac{u_1 - u_{-1}}{h+k}\right) \tag{71b}$$

These semi-discretizations are energy conservative. I.e., the corresponding forms of discrete energy:

a) finite differences:

$$\|u_n\|_2^2 = h\sum_{n<0} u_n^2 + \left(\frac{h+k}{2}\right)u_0^2 + k\sum_{n>0} u_n^2 \tag{72a}$$

b) finite elements:

$$\|u_n^*\|_2^2 = \frac{h}{3}\sum_{n<0}(2u_n^2 + u_n u_{n+1}) + \frac{k}{3}\sum_{n\geq 0}(2u_n^2 + u_n u_{n+1}) \tag{72b}$$

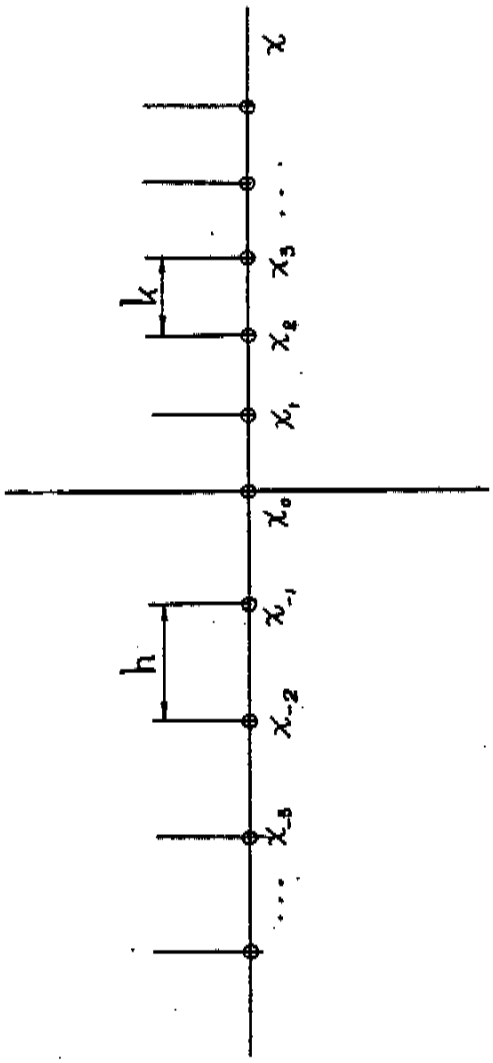

Figure 8

are constant for solutions which satisfy (71)

Because of the difference in numerical propagation properties in the two media $x>0$ and $x<0$, reflection occurs when a solution passes through the interface $x=0$.

Four types of fundamental solutions may exist near the interface point $x=0$. These are the forward and backward solutions in $x<0$ (where $\Delta x = h$), and the forward and backward solutions in $x>0$ (where $\Delta x = k$). Since no reflection is assumed to occur to the right of the origin, only the first three may exist, which we denote by $\{p_n\}$, $\{q_n\}$ and $\{r_n\}$ respectively.

While the first two simply satisfy (19) (20), $\{r_n\}$ satisfies (19) with h replaced by k.

It then becomes an easy matter to proceed as before, taking the t-Fourier transform of (71) to obtain:

$$\rho(\Omega) = -\frac{\sqrt{1-(\Omega/\Omega_{c,L})^2} - \sqrt{1-(\Omega/\Omega_{c,R})^2}}{\sqrt{1-(\Omega/\Omega_{c,L})^2} + \sqrt{1-(\Omega/\Omega_{c,R})^2}} \qquad (73)$$

where $\Omega_{c,L}$ and $\Omega_{c,R}$ are the cut-off frequencies to the left and to the right of $x=0$ i.e., those corresponding to $\Delta x = h$ and $\Delta x = k$, respectively.

It is shown in [26] and [28] that these expressions of the reflection ratio are precisely those which ensure discrete energy flow conservation through the mesh interface point.

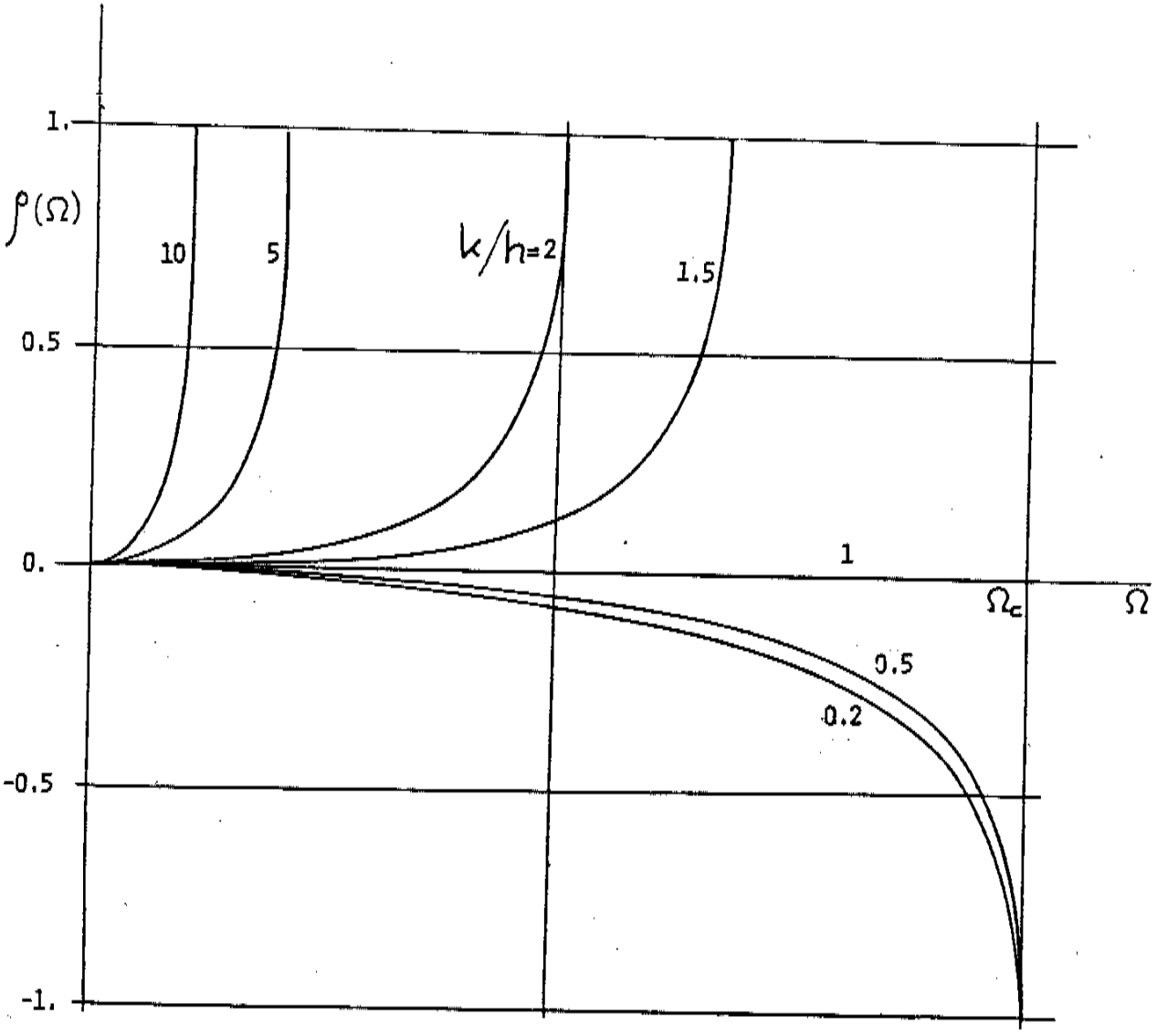

Figure 9: Reflection ratio at the mesh interface point of figure 8
Finite difference and Finite element cases.

This is one of the cases where solutions corresponding to $|\Omega| > \Omega_c$ may exist. This occurs in mesh coarsening ($k > h$): sinusoidal solutions of $\{p_n\}$ type in $x < 0$ which correspond to

$$\Omega_{c,R} < |\Omega| < \Omega_{c,L}$$

are reflected at the interface with $|\rho(\Omega)| = 1$.
To the resulting solution in $x > 0$ correspond an $|\hat{E}_1(\Omega)| < 1.$, thus an exponentially decaying envelope as $|\hat{E}_1|^n$, and no energy is propagated inside of the half space to the right; all the energy is of course reflected toward $x < 0$, as a solution of $\{q_n\}$ type.

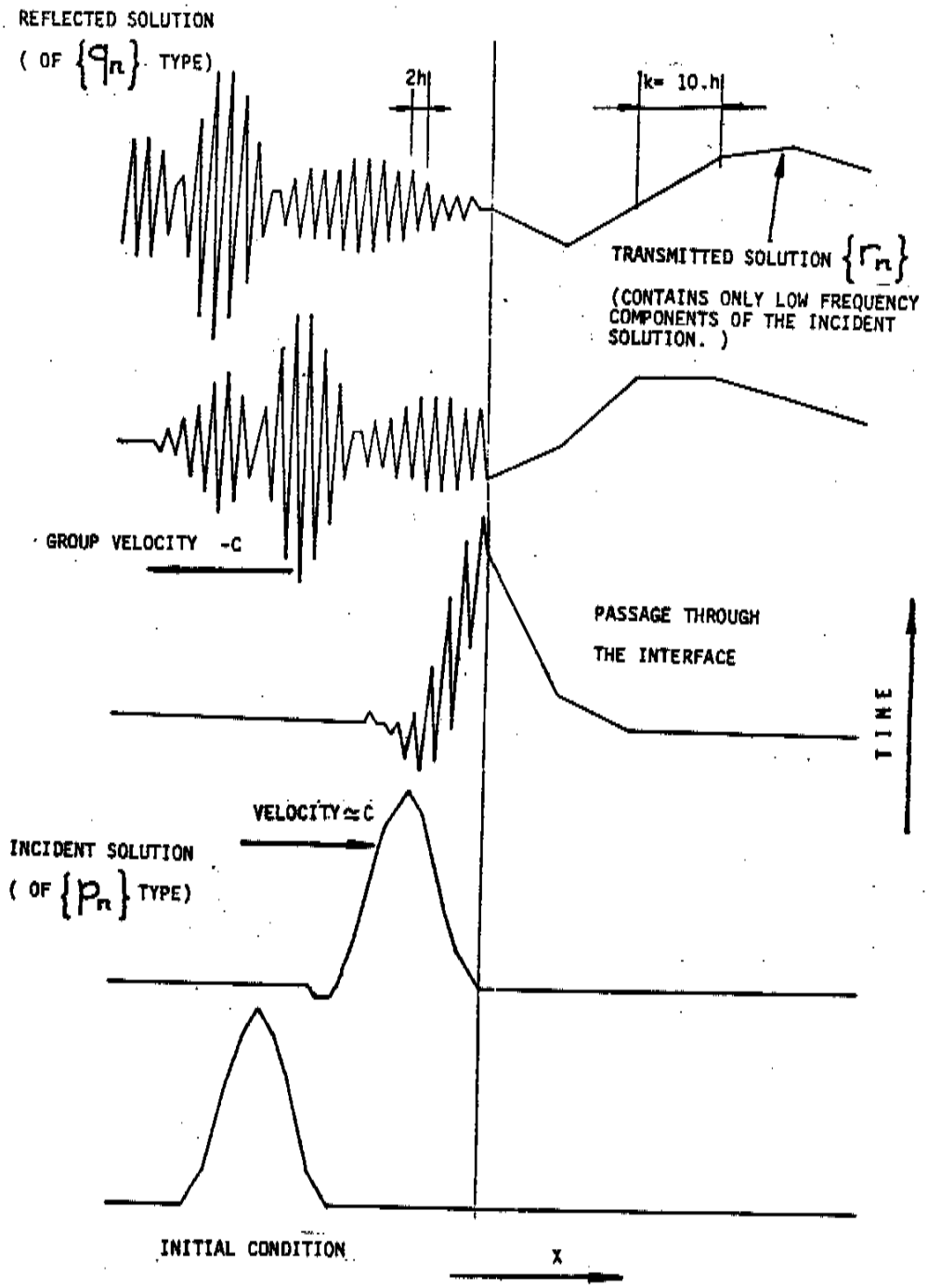

Figure 10: Illustration of reflection at the interface point
Mesh coarsening case : k/h= 10
Finite difference case.

13- STABILITY

Finally, we briefly outline the essence of an interresting relationship between group velocity and stability that was recently put to light by Trefethen (1982): Consider a conservative discretization of $U_t + c\,U_x = 0$,in a domain which is limited by a boundary. A special discrete treatment need be used near the boundary point, and stability analyses of the global algorithm must take this into account.

A "classical" , not simple at all, formulation of global stability conditions based on properties of eigensolutions of the scheme had been given by Gustafsson, Kreiss and Sundstrom(1972)- see also Strikwerda (1978). The new result of Trefethen shows that one of the Gustafsson Kreiss Sundstrom stability conditions is equivalent to stating that the discretization at the boundary may not support a sinusoidal mode in the interior domain whose group velocity points away from the boundary. Thus the corresponding (unstable) eigensolutions in the Gustafsson Kreiss Sundstrom theory are those which would allow the numerical boundary equations to generate energy which can be propagated away from the boundary inside of the computational domain.

REFERENCES

[1] Birkhoff, G. and V. A. Dougalis (1975), "Numerical Solution of Hydrodynamic Problems" - in ADVANCES IN COMPUTER METHODS FOR PARTIAL DIFFERENTIAL EQUATIONS - R. Vichnevetsky (ed.), pub. AICA, New Brunswick, NJ.

[2] Brillouin, L. (1946), "Wave Propagation in Periodic Structures" - McGraw Hill, New York.

[3] Brillouin, L. (1960), "Wave Propagation and Group Velocity" - Academic Press Inc., New York, New York.

[4] Browning, G., H. O. Kreiss and J. Oliger (1973), "Mesh Refinement" Math. Comp. 27, pp. 29-39.

[5] Carver, M. B. and H. W. Hinds (1978), "The Method of Lines and the Advective Equation" - SIMULATION - Vol. 31, pp. 59-69.

[6] Carver, M. B. and W. E. Schiesser (1980), "Biased upwind difference approximations for first order hyperbolic partial differential equations" - 73d. Annual Meeting of the American Institute of Chemical Engineers.

[7] Chin, R. C. Y., and G. W. Hedstrom (1978), "A Dispersion Analysis for Finite Difference Schemes: Tables of Generalized Airy Functions" - Mathematics of Computation 32, pp. 1163-1170.

[8] Faddeyeva, V. N. (1949). "The method of straight lines in the application to certain Boundary Problems" - Trudy Matematicheskogo Instituta (Transactions Mathematical Institute, USSR), Vol. 28, pp. 73,103, (English Translation - FTD, Wright Patterson AFB - #66-163 - July 1967).

[9] Gustafsson, B., H. O. Kreiss and A. Sundstrom (1972), "Stability theory for difference approximations for mixed initial boundary value problems II, Math. Comp. 26, pp. 649-685.

[10] Hamilton, W. R. (1839), Proc. Roy. Irish Acad. 1 267,341.

[11] Hyman, J. N. (1979), "A Method of Lines Approach to the Numerical Solution of Conservation Laws" - in R. Vichnevetsky and R. Stepleman (ed.), ADVANCES IN COMPUTER METHODS FOR PARTIAL DIFFERENTIAL EQUATIONS III - IMACS - New Brunswick, NJ.

[12] Kreiss, H. O. and J. Oliger (1972), "Comparison of Accurate Methods for the Integration of Hyperbolic Equations" - Tellus - Vol. XXIV, No. 3, pp. 199-215.

[13] Kreiss, H. O. and J. Oliger (1973), "Methods for the Approximate Solution of Time Dependent Problems" - Garp Publication Series, No. 10, February.

[14] Rayleigh (J. W. Strutt, Baron Rayleigh)(1877), "Theory of Sound" - Vol 1. The MacMillan Company, London. 2nd ed.(1894) reprinted by Dover Publications, Inc., New York in 1945.

[15] Roache, P. J. (1972), "Computational Fluid Dynamics" - Hermosa Press, Albuquerque, N.M.

[16] Sommerfeld (1914), "About the propagation of light in dispersive media" (in German) Ann. Phys. 4, 44, English translation reprinted in [Brillouin (1960) ref. [3] above].

[17] Strikwerda, J. C. (1978), "Initial Boundary Value Problems for the Method of Lines" - ICASE Report 78-16, Nasa Langley Res. Center, Hampton, Virginia.

[18] Swartz, B. and B. Wendroff (1974), "The Relative Efficiency of Finite Difference and Finite Element Methods. Hyperbolic Problems and Splines" - Siam J. Numer, Analysis, Vol. II, No. 5, pp. 979-993.

[19] Swartz, B. (1975), "Comparing Certain Classes of Difference and Finite Element Methods for a Hyperbolic Problem" - in ADVANCES IN COMPUTER METHODS FOR PARTIAL DIFFERENTIAL EQUATIONS, publ. AICA, New Brunswick, NJ.

[20] Thomée, V. (1969), "Stability for Partial Difference Operators" - Siam Review - Vol. II, No. 2, pp. 152-195.

[21] Thomée, V. (1973), "Convergence Estimates for Semi-Discrete Galerkin Methods for Initial Value Problems" - in Ansorge and Tornig, ed. Lecture Notes in Mathematics, No. 333, Springer Verlag.

[22] Trefethen, L. (1982), "Group Velocity in Finite Difference Schemes" - SIAM Review, 24, pp. 113-136.

[23] Vichnevetsky, R. (1977), "Mean Squared Accuracy of Numerical Approximations of Hyperbolic Equations" - Mathematics and Computers in Simulation XIX, pp. 159-168 - North Holland Publishing Co.

[24] Vichnevetsky, R. (1980), "Propagation Characteristics of Semi-Discretizations of Hyperbolic Equations" - Mathematics and Computers in Simulation XXII, pp. 98-107 - North Holland Publishing Co.

[25] Vichnevetsky, R. (1981a), "Energy and group velocity in semi-discretization of hyperbolic equations" - Mathematics and Computers in Simulation, Vol. XIXIII, North Holland Publishing Co.

[26] Vichnevetsky, R. (1981b), "Propagation through Numerical Mesh Refinement for Hyperbolic Equations" - Mathematics and Computers in Simulation, Vol. XXIII, North Holland Publishing Co.

[27] Vichnevetsky, R. (1982a), "Energy and Group Velocity in a Finite Element Approximation of Hyperbolic Equations" - Report NAM 202 - Department of Computer Science, Rutgers University, New Brunswick, NJ.

[28] Vichnevetsky, R. (1982b), "Propagation through Mesh Refinement and Boundaries of Finite Element Approximations of Hyperbolic Equations" - Report NAM 203 - Department of Computer Science, Rutgers University, New Brunswick, NJ.

[29] Vichnevetsky, R. and A. W. Tomalesky (1971), "Spurious Wave Phenomena in Numerical Approximations of Hyperbolic Equations" - Proceedings, Fifth Annual Princeton Conference on Information and Systems Science, March.

[30] Vichnevetsky, R. and B. Peiffer (1975), "Error Waves in Finite Element and Finite Difference Methods for Hyperbolic Equations" in ADVANCES IN COMPUTER METHODS FOR PARTIAL DIFFERENTIAL EQUATIONS, publ. AICA, New Brunswick, NJ.

[31] Vichnevetsky, R. and F. De Schutter (1975), "A Frequency Analysis of Finite Difference and Finite Element Methods for Initial Value Problems" in ADVANCES IN COMPUTER METHODS FOR PARTIAL DIFFERENTIAL EQUATIONS, publ. AICA, New Brunswick, NJ.

[32] Vichnevetsky, R. and J. B. Bowles (1982),"Fourier Analysis of Numerical Approximations of Hyperbolic Equations" - SIAM (Book in the Studies in Applied Mathematics Series), Philadelphia, PA.

[33] Vichnevetsky, R. and E. Sciubba (1981), "Non reflecting upstream boundaries for hyperbolic equations" - in ADVANCES IN COMPUTER METHODS FOR PARTIAL DIFFERENTIAL EQUATIONS IV, Publ. IMACS, Rutgers University, New Brunswick, NJ.

[34] Wesseling, P. (1972), "Accuracy of Third Order Predictor Corrector Difference Schemes for Hyperbolic Problems" - AIAA Journal, Vol. 10, No. 7 (July).